Molecular Investigations of Selected Spike Protein Mutations in SARS-CoV-2: Delta and Omicron Variants and Omicron BA.2 Sub Variant

Urmi Roy[*]

[*]Department of Chemistry & Biomolecular Science

Clarkson University

8 Clarkson Avenue, Potsdam, NY 13699-5820, United States

[*]To whom correspondence should be addressed. E-mail: urmi@clarkson.edu; Phone: 315/212-7346; ORCID iD: https://orcid.org/0000-0003-0928-0574

Abstract:

Among the multiple SARS-CoV-2 variants recently reported, the delta variant has generated most perilous and widespread effects. Another variant, omicron, has been identified specifically for its high transmissibility. Omicron contains numerous spike (S) protein mutations and in numbers much larger than those of its predecessor variants. BA.2, a sub variant of omicron, has recently emerged with more spreadable infectivity as compared to the original omicron species. BA.2 also contains several new and additional mutations in its spike protein, and represents the globally most prevalent form of SARS-CoV-2 at the present time.

In this report we discuss some essential structural aspects and time-based structure changes of a selected set of spike protein mutations within the delta and omicron variants, including those of omicron BA.2. The expected impact of multiple-point mutations within the spike protein's receptor-binding domain (RBD) and S1 are also discussed. It is expected that the structural data discussed in this report will be helpful to identify drug targets and to neutralize antibodies for the evolving variants/sub variants of SARS-CoV-2.

Keywords: BA.2; SARS-CoV-2; spike protein; structural biochemistry; sub variant; virus structure

1. Introduction

Since WHO declared a Public Health Emergency due to SARS-Cov-2 in January 2020 [1], several different variants of corona virus has emerged. Among these variants, the delta strain has been reported to be particularly aggressive due to its fast transmissibility and strong infectivity. The delta variant, also known as the B.1.617.2 strain, was first identified in India, and n was listed among the CDC's "Variants of Concern" [2]. The highly contagious B.1.1.529 strain, omicron, was first identified in South Africa in December 2021 [3], and the presence of numerous spike (S) protein mutations in omicron makes this variant extremely contagious and highly transmissible. More recently the BA.2 sub variant of omicron, containing many additional mutations in its S protein has become a predominant COVID 19 species worldwide [4]. These mutations within the recent SARS-COV-2 variants and sub variant BA.2 are listed in Table SI1.

As new variants/sub variants of SARS-CoV-2 continue to emerge, they are likely to be associated with more epitope escape mutations with unknown mutations of greater epidemiological fitness. High performance computational tools have the potential of aiding the ongoing efforts to identify the proper therapeutic targets for these pathogenic variants. In this regard, structure-based computational immunology and bioinformatics based methods of immuno-engineering play a critical role in detecting proper drug targets as well as in designing new vaccines [5-7].

In our previous reports we have discussed time-based structures of various immunologically significant proteins and their structure-functions relationships [8-10]. We have also reported the impacts of mutations on the receptor binding domain (RBD) of SARS-CoV-2 [11,12]. Recently we have also examined the impact of Zn ion coordinated Angiotensin II peptides on the spike 1 (S1)-angiotensin converting enzyme-2 (ACE2) receptor binding [13]. In

the present communication, we will analyze most of the RBD mutations observed in delta and omicron variants and omicron sub variant BA.2, and we will also determine their structural changes and stability as functions of time. Results for the time based structures of wt SARS-CoV-2 S1 and the S1 mutations within the delta, omicron, and BA.2 will be included.

Moreover, initially we have started to explore a possible combination of delta and omicron variants and very recently a few cases of deltacron recombinant species is identified in some countries [14]. The RBD and S1 mutations within the mu and delta-omicron variants are also briefly explored here as well. Within the delta variant residue 681 is mutated to P681R. However in omicron variant this is P681H. We have kept P681R in the S1 of combined delta-omicron variant. Another variant, mu was briefly discussed in this report that was described as "Variants Being Monitored" by CDC [2].

2. Materials and Methods

The spike (S) protein of the SARS CoV-2 comprised of two subunits, S1 and S2. This paper is centered on the wt and recent mutant variants of the RBD and S1 subunit. The 6M0J.PDB was selected for the wt RBD simulations [15]. Starting from the wt RBD structure, the mutant variants were generated using the VMD mutator plugin graphical user window (GUI). We have analyzed the selected S1 RBD mutations within the B.1.617.2 strain, the delta variant and the B.1.1.529 strain, the omicron variant, along with an exploration of the RBD BA.2. The B.1.621 strain, also known as the mu variant and another possible combination of the delta and omicron variants has been briefly described. The structural analyses of these last two species were described in the Supplementary Information (SI).

The I Tasser server was used to model the structure of SARS-CoV-2 S1 [16]. The wt S1 was prepared based on the 6VYB.PDB; chain B [17]. Due to the lack of experimental data, part of the protein sequences have still been missing in the published literature, making those sequences difficult to model; some of these missing sequences have been based here on the PDB structure 6ZP2 and other resources reported elsewhere [4,18]. The selected RBD and S1 mutations used in these simulation experiments have been listed in Supporting Table SI.1. Some mutations are updated later.

For the simulation purpose we have used the NAMD, VMD and quikMD packages [19-21]. The implicit solvation system was used with the Generalized Born Solvent-Accessible Surface Area [22]. After initial minimization, annealing and equilibration processes of the MD production run were procured using the NVT ensemble. The production run was set for 25 and 20 ns for the RBD and S1 respectively. The detailed experimental procedures have been described elsewhere [11]. The resulting data were analyzed using VMD and the figures for reporting were developed using Biovia Discovery Studio Visualizer [23]. The plots of processed data were generated using origin.

3. Results and Discussions

The RBD of 6M0J.PDB contains residues 333 to 526 AAs. The RBD mutations on 6M0J are displayed in Fig.1 A-C. Fig. 1A includes the 3 mutations within the delta/ B.1.617.2 strain selected for this study. Fig. 1B includes the 15 selected mutations within the omicron/B.1.1.529 strain and Fig. 1C displays the 18 selected mutations within the omicron BA.2 sub variant. The 3 mutations selected within the mu /B.1.621 and a potential combined strain of delta-omicron are tabulated in SI Table SI. This delta-omicron contains one additional mutation L452R from the

delta variant in addition to the omicron RBD mutations. The RBD mutations of other variants have been described in our previous report [12].

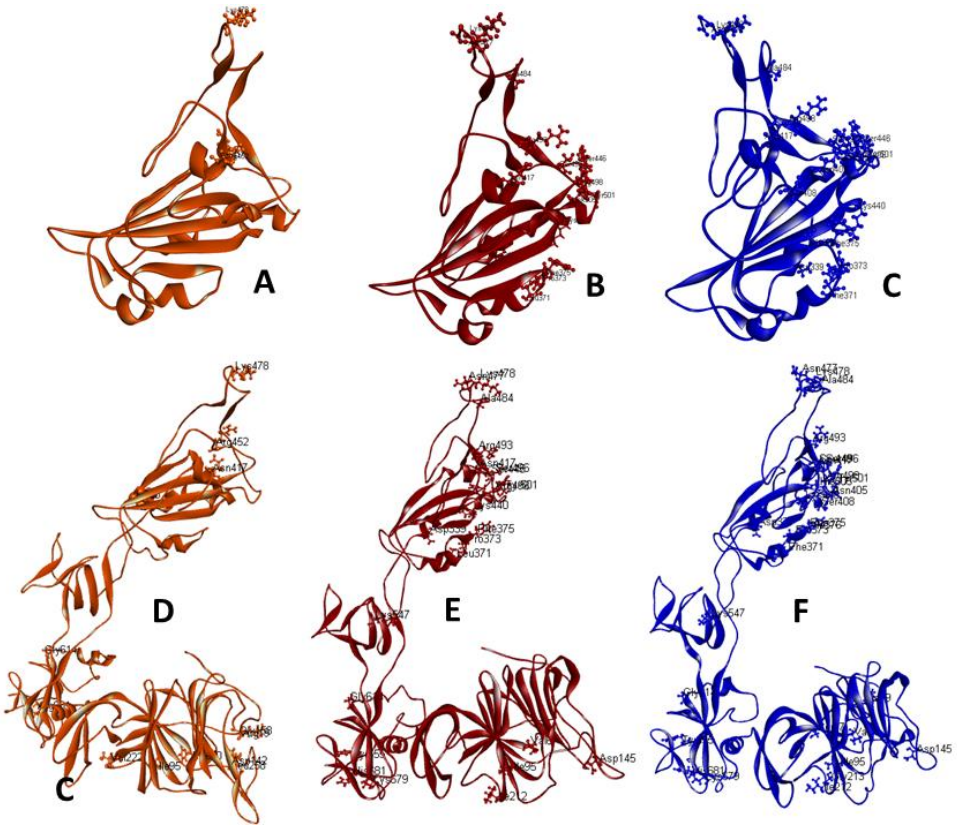

Figure 1. A-C Ribbon diagram of SARS-CoV-2 variants with selected RBD mutations. These variants are based on 6M0J structure. Displayed are the A. delta RBD with selected mutations B. omicron variant RBD with selected mutations and C. omicron BA.2 sub variant with selected RBD mutations. D-F. Ribbon diagram of SARS-CoV-2 variants with selected S1 mutations. D. delta variant with selected S1 mutations. E. omicron variant with selected S1 mutations. and F. omicron sub variant BA.2 with selected S1 mutations.

Fig. 2A illustrate the traditional RMSD plots of wt and different SARS-CoV-2 variants with selected RBD mutations; wt SARS-CoV-2 has also been included here for comparison. It is evident from this plot that delta RBD is the most stable form among all species studied here. This variant is more stable than omicron and even stable compare to its wt version. While the omicron variant is most unstable, the RBD of omicron sub variant BA.2 is quite stable. The average root mean square deviation (RMSD) of the BA.2 sub variant is slightly higher than that of the delta

variant as displayed in Fig. 2B. Fig. 2B also describes the RMSD results within the delta and omicron species. The delta variant has the lowest average RMSD values while omicron has the highest. This figure also indicates certain findings from Fig. 2A, where the omicron variant shows larger variations. Fig. 2C presents the RMSD plots of RBD mutations within different variants. The results in Figs 2C-2D suggest that the mutations in the delta variant are most stable and those of omicron are most unstable. It is possible that numerous RBD mutations within the omicron make the latter unstable; this is not the case for the RBD of omicron sub variant BA.2, where the presence of RBD mutations make this protein rather stable.

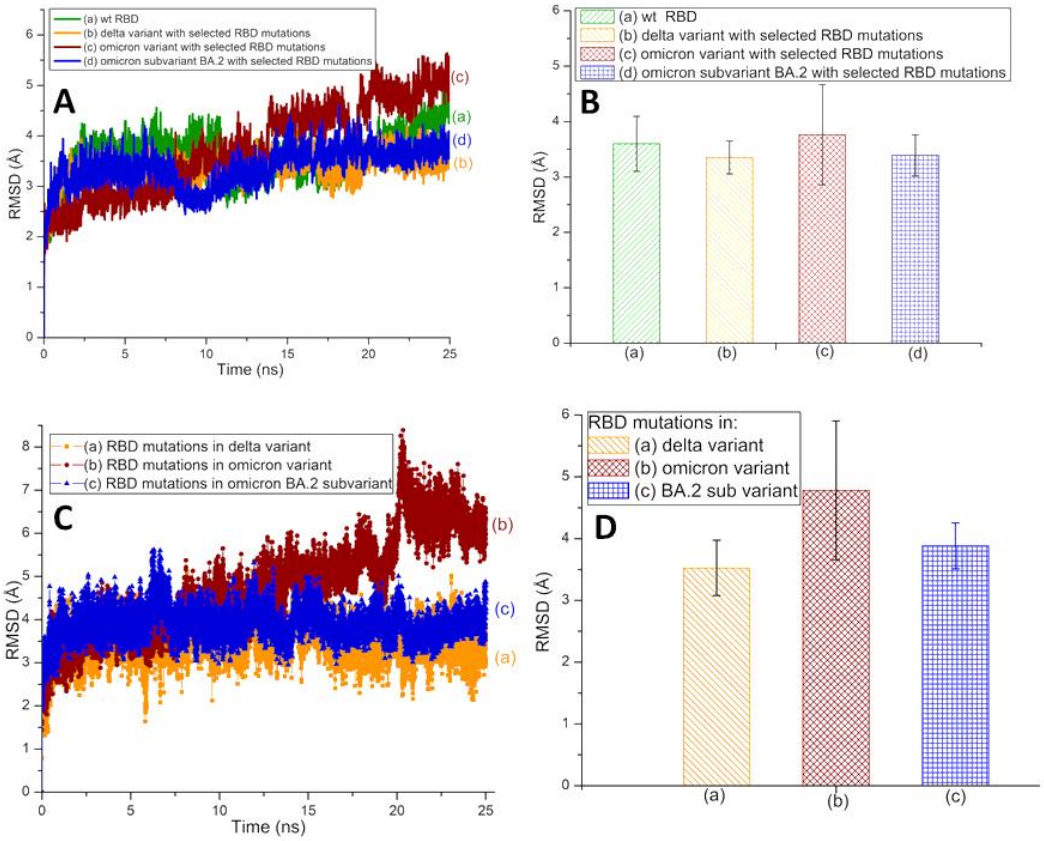

Figure 2. A. The typical RMSD plots of wt and different SARS-CoV-2 variants with selected RBD mutations. These variants are based on spike RBD, 6M0J.PDB. B The average RMSD plots of wt RBD, delta, omicron variants and BA.2 sub variant with selected RBD mutations. The average values of RMSD were taken from 25ns simulation time. These values are extracted from Fig. 1A. C. The typical RMSD plots of RBD mutations within different SARS-CoV-2 variants and sub variant. D. The average RMSD plots for SARS-CoV-2 mutations within deferent variants. These average values of RBD mutations are extracted from Fig. 1C.

Fig. 3A represents the traditional RMSD graphs of the wt and the mutant variants of SARS-CoV-2 S1 with selected mutations. Fig 3B shows the average RMSD values of the wt and variant proteins with selected S1 mutations. From these plots we can infer that the omicron variant and BA.2 sub variant with S1 mutations show higher RMSD values compare to those of the delta variant. It is also clear from Fig. 3C-D that the S1 mutations within the delta variant show the lowest degree of RMSD variations. Therefore, we can assume that delta variant is the most stable form of this virus among these variants and sub variant. Interestingly, at the same time, the S1 of BA.2 shows marginally lower RMSD (11.67Å) than delta S1 (11.76Å) though the RBD of delta (3.35Å) seems slightly more stable than the BA.2 RBD (3.39Å). The overall RMSD values of the S1 are much higher than the RBD RMSDs due to the presence of many turns and coils in the protein.

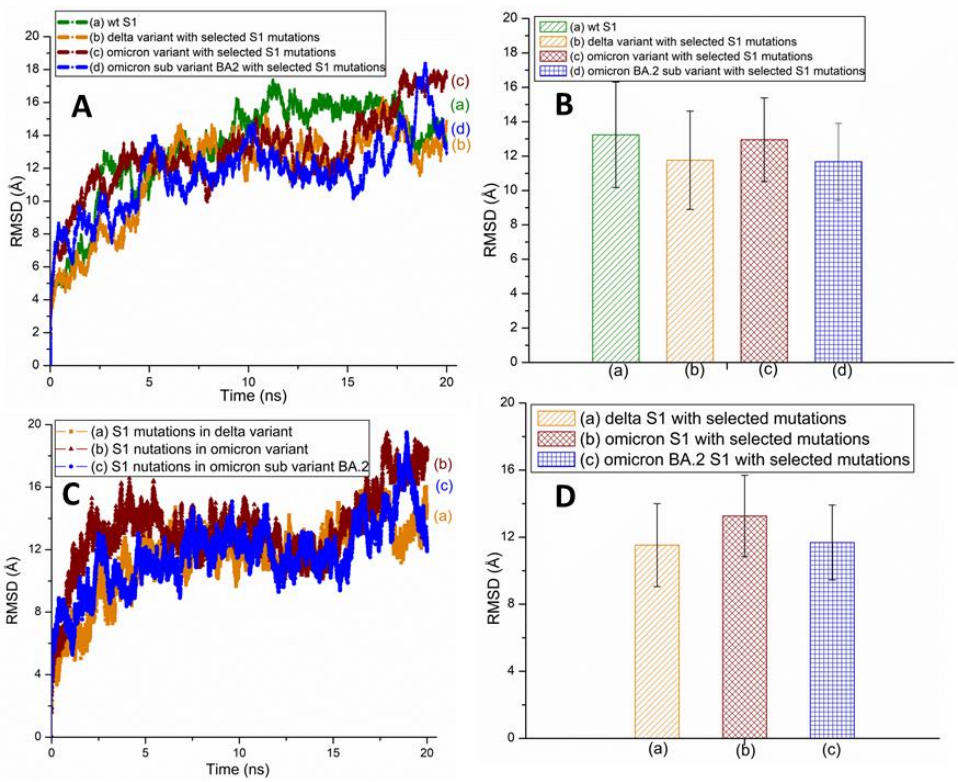

Figure 3. A. The typical RMSD plots of wt and different SARS-CoV-2 variants and sub variant with selected S1 mutations. These variants/ sub variant are based on model protein of S1. B The average RMSD plot of wt S1, delta and omicron variants and BA.2 sub variant with selected S1 mutations. The

average RMSD values were measured from 20ns simulation time. These values were extracted from Fig. 3A. C. The typical RMSD plots of S1 mutations within different SARS-CoV-2 variants and sub variant. D. The average RMSD plots for SARS-CoV-2 mutations within deferent variants and sub variant. These average values were extracted from Fig. 3C.

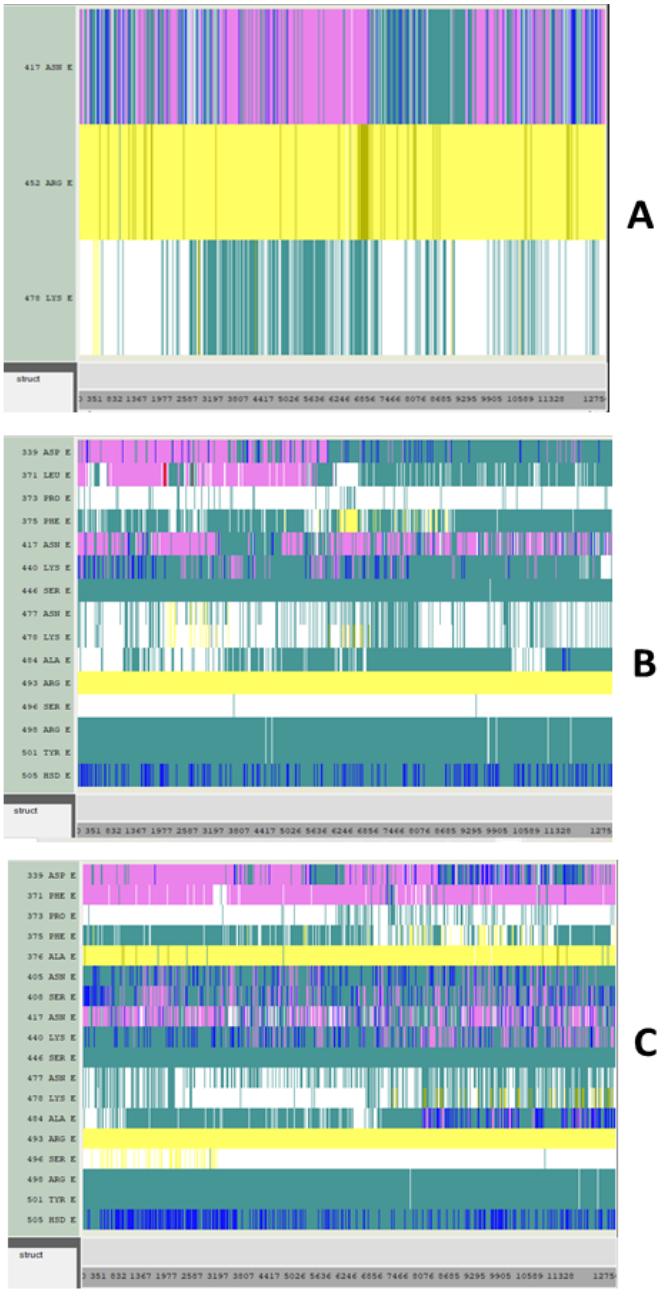

Figure 4. Time based secondary structure changes of SARS-CoV-2 mutant variants and sub variant (A) delta, (B) omicron and (C) omicron BA.2 sub variant with selected RBD mutations. The vertical axis represents the mutated residues and the horizontal axis represents the simulation time scale. These secondary structure changes were recorded for 25ns.

Results of time based secondary structure analyses of different RBDs are displayed in Fig. 4. The secondary structure of K417N and L452R mutations in delta variant are stable compared to T478K (Fig. 4A). In the omicron variant most of the mutations are unstable including G339D, S371L, S375F, N440K, S477N and T478K, which, in combination, make the omicron RBD measurably unstable (Fig. 4B). In BA.2 sub variant R408S, T478K and E484A residues seems very stable whereas residues G339D and G496S appear unstable (Fig.4C). These results, suggest an overall high stability of the delta RBD. Based on its RBD, the sub variant BA.2 is also a stable protein and omicron RBD is most unstable among these three RBDs.

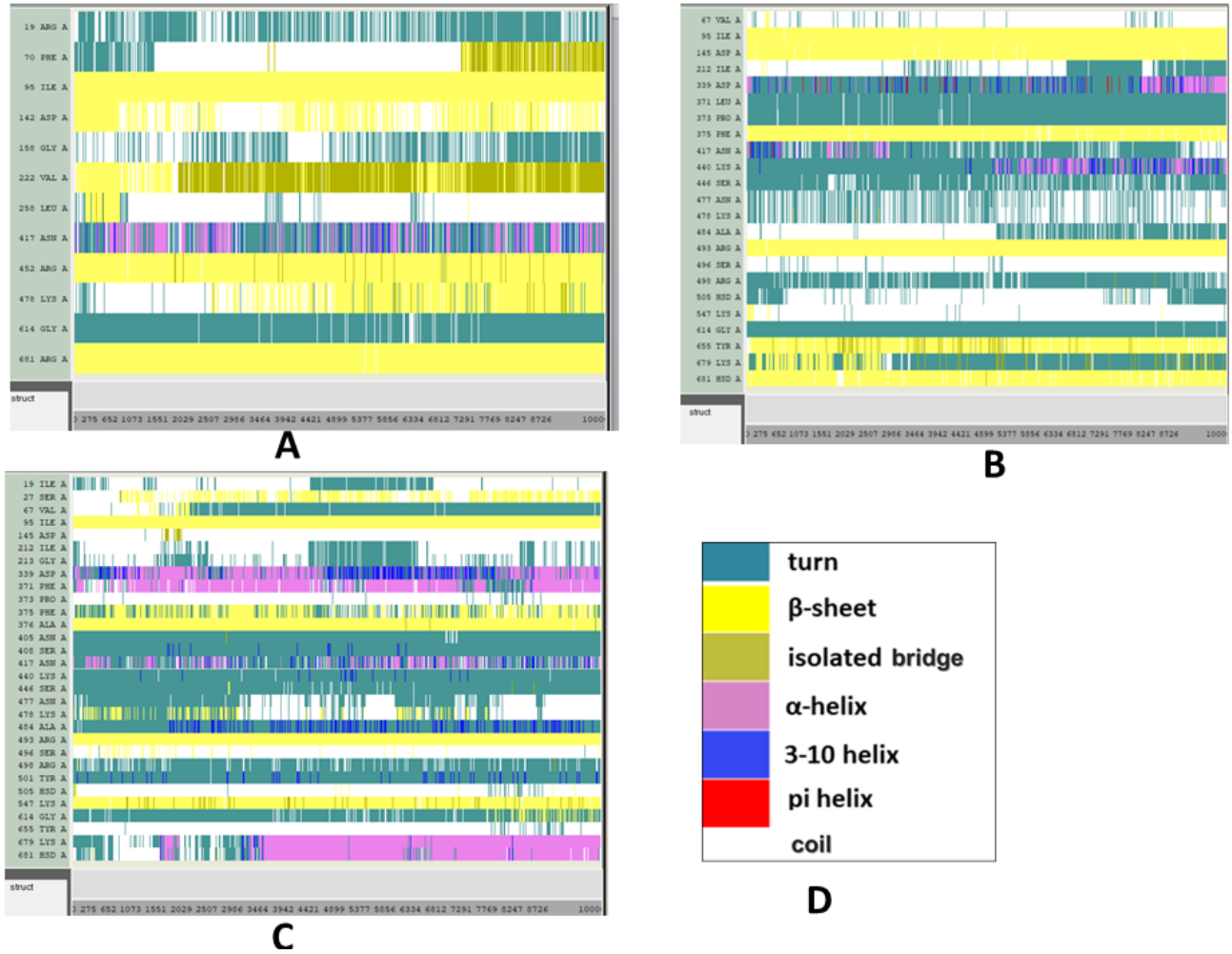

Figure 5. The Secondary structure changes of SARS-CoV-2 wt and mutant S1 with selected mutations. A. delta B. omicron variants and C. omicron sub variant BA.2. These structural changes were recorded

for 20ns. D. Color code explanation of proteins' secondary structures. These are the default color codes generated by VMD graphical user interface.

Fig. 5 illustrates the secondary structure changes of SARS-CoV-2 S1 of delta, and omicron variants and BA.2 sub variant with selected mutations. The delta S1 appears quite stable (Fig.5A). No major changes in the stability or fluctuations within the secondary structures are observed for this variant. V70F and T478K residues also seem quite stable during the simulation timescale as the turns and coils of these species are converted into beta sheets. In the case of omicron S1, though residues G339D and N440K seem stable with time, fluctuations are observed in the mutated residues A67V, L212I, K417N and T547K (Fig. 5B). For the BA.2 sub variant (Fig.5C), residues V47 and T478K seem unstable as their beta sheets are converted into turns and coils. On the other hand, residues F375, 479-81 are converted to alpha helices and beta sheets from their turns/coils phases, respectively. The stability analyses of S1 secondary structure mimics those of the RBD secondary structures, and suggests that delta is the most stable variant, while the BA.2 sub variant is more stable than omicron.

The average solvent accessible surface area (SASA) values for each of the RBD and S1 mutations within the SARS-CoV-2 variants and sub variants are plotted in Fig.6. These results are average SASA values obtained from the simulation time scale. The SASA values are calculated using the VMD timeline window. It should be noted in this context that the severity of certain disease largely depends on the buried or exposed nature of the underlying mutated residues [24]. In Fig. 6A, the highest SASA values are observed in L452R within the RBD of delta variant, which suggests that this residue has a comparably large solvent accessible surface. The SASA values may increase due to partial unfolding caused by residue mutation.

Among the three species we have studied here, the L452R mutation is only observed in the delta variant. Since mutated residue R is hydrophilic and surface exposed, the structural

rearrangements or conformational deviations may possible in this case. Published report suggests that L452R within the delta variant strongly interacts with ACE2 [25]. T478K within delta variant also shows considerably high SASA value. As positively charged K^+ impact the electrostatic surface area, this residue may manifest stronger interactions with the receptor [26]. In delta RBD, only one residue shows considerably lower SASA values indicating that this buried residue K417N is quite stable in nature. However, if surface exposed residues on the RBD form stable interactions with the ACE2 receptor as in the case of delta, where the mutant L452R strongly bind to the ACE2 receptor making delta RBD quite stable. Thus it could be possible that the L452R and T478K within the delta variant may have a stronger stabilizing effect [12,27]. Although T478K was not present in any previously identified variants, this mutation is observed in all the variants and sub variant we studied in this report. It is possible that the greater mutational fitness of the delta variant may be due to L452R or a combination of a number of residue mutations.

In the case of omicron RBD, as displayed in Fig. 6B, despite the presence of fewer buried residues with lower SASA values, majority of the mutated residues have greater SASA values; this suggests the possibility of making this protein quite unstable as S protein of omicron variant demonstrated decreased receptor interactions [28].

The omicron variant contains more mutations than delta and some of them are at the ligand-receptor interfacial region, while the stronger binding interactions between L452R and ACE2 receptor make delta variant somewhat unique. Hydrogen bond formation between residue G493 of delta with ACE2 contributes to it stronger structure [25]. Furthermore, it is possible that most of the mutations present in the omicron variant are counteracted by neutralizing antibodies, while at the same time, L452R in delta is considered as antibody neutralizing escape mutation.

In the case of BA.2, as displayed in Fig.6C the slightly higher numbers of buried residues (with lower SASA values) possibly make this sub variant more stable than original omicron. Usually, the buried residues present within the core of the protein are the most stable part of a protein. The surface exposed residues with greater SASA values are likely to be comparatively less stable unless the surface exposed residues form stronger receptor interactions.

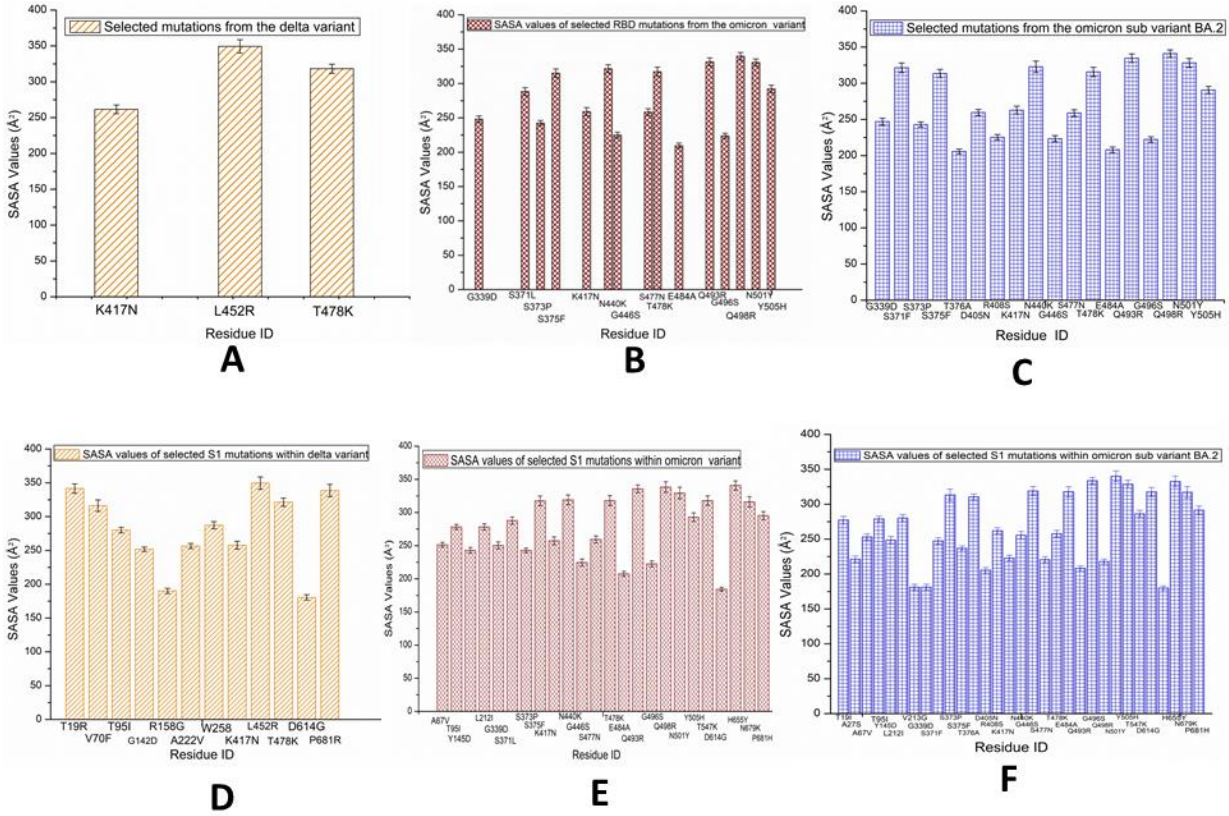

Fig. 6. Average SASA values of SARS-CoV-2 RBD and S1 with selected mutations. A-C. RBD of A. delta B. omicron RBD and C. omicron sub variant.BA.2. D-E. S1 of A. delta B. omicron and C. omicron sub variant.BA.2.

The SASA values of S1 mutations are displayed in Fig 6D-F, where the findings of the corresponding RBDs are detected again. The delta has a number of buried residues, but here the surface exposed residues have strong interactions with ACE2. Despite the many buried residues of omicron, the numbers of surface exposed residues are greater than the buried residues in this

case. S1 of sub variant BA.2 has more buried residues than those of the S1 of omicron variant. It is likely that most of the surface exposed residues in the omicron variant are loosely attached to the ACE2 receptor. Currently there are no readily available experimental results for the BA.2 sub variant. It could be possible that the surface exposed residues within sub variant BA.2 bind more strongly to the ACE2 receptor than omicron variant. This sub variant may have antibody neutralizing escape mutants and thus, may emerge as a strong form of the virus [29,30]. Nonetheless, according to the RMSD data and the time-based secondary structure analyses presented here, the delta is currently most stable, sub variant BA.2 also is quite stable among the three forms we have studied. The delta-omicron species also shows low RMSD values (Fig. SI. 2).

4. Conclusions

The simulation data reported here indicate that delta is the most stable form of COVID 19 and the omicron BA.2 sub variant is also quite stable among the selected forms we have studied. We expect that the structural data discussed in this paper will be useful to identify drug targets and neutralizing antibodies for emerging SARS-CoV-2 variants or sub variants with newer escape mutations. We also hope that by contributing to the literature on SARS-CoV-2, the present manuscript will serve to help the ongoing efforts to overcome the COVID 19 pandemic in some ways .

Omicron sub variant BA.2 has been known as “stealth omicron” as this sub variant was initially difficult to identify from the delta variant using traditional testing procedures. Recently, a combination of sub variants BA.1 and BA.2 has been reported. This hybrid or recombinant variant is also known as sub variant XE [31]. Several omicron sub variants including BA.3,

BA.4, BA.5 and two versions of omicron variant BA.2.12.1 and BA.2.12 have also been identified. As the mRNA virus is highly adaptable and environmentally fit, it is possible that newer sub versions of variants/sub variants would arise with new functional epitopes with antibody neutralizing escape mutations.

Conflict of interest statement

The author declares no conflict of interest.

Acknowledgments

The author acknowledges utilization of the following simulation and visualization software packages: 1) NAMD and 2) VMD: NAMD and VMD, developed by the Theoretical and Computational Biophysics Group in the Beckman Institute for Advanced Science and Technology at the University of Illinois, Urbana-Champaign. 3) Discovery Studio Visualizer: Dassault Systèmes BIOVIA, Discovery Studio Modeling Environment, San Diego, CA: Dassault Systèmes (2015).

References

1. WHO, Weekly epidemiological update. Available online: https://www.who.int/publications/m/item/weekly-epidemiological-update---23-february-2021. (accessed on 25 February 2021).
2. Centers for Disease Control and Prevention, SARS-CoV-2 Variant Classifications and Definitions. Available online: https://www.cdc.gov/coronavirus/2019-ncov/variants/variant-info.html#Interest. (accessed on Accessed June 22, 2021, July 26, 2021, December7, 2021, April 26, 2022).
3. Science Brief: Omicron (B.1.1.529) Variant. Available online: https://www.cdc.gov/coronavirus/2019-ncov/science/science-briefs/scientific-brief-omicron-variant.html (accessed on February 18, 2022).
4. Variant: 21L (Omicron) also known as BA.2. Available online: https://covariants.org/variants/21L.Omicron (accessed on March 22, 2022).
5. Haspel, N.; Jang, H.; Nussinov, R. Active and Inactive Cdc42 Differ in Their Insert Region Conformational Dynamics. *Biophys. J.* **2021**, *120*, 306-318.
6. Lampe, A.T.; Puniya, B.L.; Pannier, A.K.; Helikar, T.; Brown, D.M. Combined TLR4 and TLR9 agonists induce distinct phenotypic changes in innate immunity in vitro and in vivo. *Cellular immunology* **2020**, *355*, 104149.
7. Schneidman-Duhovny, D.; Wolfson, H.J. Modeling of Multimolecular Complexes. *Methods Mol. Biol* **2020**, *2112*, 163-174.
8. Roy, U. Structural Characterizations of the Fas Receptor and the Fas-Associated Protein with Death Domain Interactions. *The Protein J.* **2016**, *35*, 51-60.
9. Roy, U. 3D Modeling of Tumor Necrosis Factor Receptor and Tumor Necrosis Factor-bound Receptor Systems. *Mol. Inform* **2019**, *38*, e1800011.
10. Roy, U. Structural and molecular analyses of functional epitopes and escape mutants in Japanese encephalitis virus envelope protein domain III. *Immunol Res* **2020**, *68*, 81-89.
11. Roy, U. Role of N501Y mutation in SARS-CoV-2 spike proteinstructure. *Preprints, 2021060238* **2021**.
12. Roy, U. Comparative Structural Analyses of Selected Spike Protein-RBD Mutations in SARS-CoV-2 Lineages. *bioRxiv* **2021**, 2021.2006.2023.449639.
13. Fatouros, P.R.; Roy, U.; Sur, S. Modeling Substrate Coordination to Zn-Bound Angiotensin Converting Enzyme 2. *bioRxiv* **2021**, 2021.2003.2027.437352.
14. Cyprus reportedly discovers a Covid variant that combines omicron and delta. Available online: https://www.cnbc.com/2022/01/08/cyprus-reportedly-discovers-a-covid-variant-that-combines-omicron-and-delta.html (accessed on January 2022).
15. Huo, J.; Zhao, Y.; Ren, J.; Zhou, D.; Duyvesteyn, H.M.E.; Ginn, H.M.; Carrique, L.; Malinauskas, T.; Ruza, R.R.; Shah, P.N.M.; et al. Neutralization of SARS-CoV-2 by Destruction of the Prefusion Spike. *Cell host & microbe* **2020**, *28*, 445-454.e446.
16. Yang, J.; Zhang, Y. I-TASSER server: new development for protein structure and function predictions. *Nucleic Acids Res* **2015**, *43*, W174-181.
17. Walls, A.C.; Park, Y.J.; Tortorici, M.A.; Wall, A.; McGuire, A.T.; Veesler, D. Structure, Function, and Antigenicity of the SARS-CoV-2 Spike Glycoprotein. *Cell* **2020**, *181*, 281-292.e286.
18. Xiong, X.; Qu, K.; Ciazynska, K.A.; Hosmillo, M.; Carter, A.P.; Ebrahimi, S.; Ke, Z.; Scheres, S.H.W.; Bergamaschi, L.; Grice, G.L.; et al. A thermostable, closed SARS-CoV-2 spike protein trimer. *Nature structural & molecular biology* **2020**, *27*, 934-941.
19. Humphrey, W.; Dalke, A.; Schulten, K. VMD: Visual molecular dynamics. *J. Mol. Graph.* **1996**, *14*, 33-38.

20. Phillips, J.C.; Braun, R.; Wang, W.; Gumbart, J.; Tajkhorshid, E.; Villa, E.; Chipot, C.; Skeel, R.D.; Kale, L.; Schulten, K. Scalable molecular dynamics with NAMD. *J. Comput. Chem* **2005**, *26*, 1781-1802.
21. Ribeiro, J.V.; Bernardi, R.C.; Rudack, T.; Stone, J.E.; Phillips, J.C.; Freddolino, P.L.; Schulten, K. QwikMD - Integrative Molecular Dynamics Toolkit for Novices and Experts. *Scientific reports* **2016**, *6*, 26536.
22. Tanner, D.E.; Phillips, J.C.; Schulten, K. GPU/CPU Algorithm for Generalized Born/Solvent-Accessible Surface Area Implicit Solvent Calculations. *J. Chem. Theory Comput.* **2012**, *8*, 2521-2530.
23. Dassault Systèmes BIOVIA *Discovery Studio Modeling Environment, San Diego, CA: Dassault Systèmes (2015).*
24. Savojardo, C.; Manfredi, M.; Martelli, P.L.; Casadio, R. Solvent Accessibility of Residues Undergoing Pathogenic Variations in Humans: From Protein Structures to Protein Sequences. *Frontiers in molecular biosciences* **2020**, *7*, 626363.
25. Socher, E.; Heger, L.; Paulsen, F.; Zunke, F.; Arnold, P. Molecular dynamics simulations of the delta and omicron SARS-CoV-2 spike - ACE2 complexes reveal distinct changes between both variants. *Computational and structural biotechnology journal* **2022**, *20*, 1168-1176.
26. Di Giacomo, S.; Mercatelli, D.; Rakhimov, A.; Giorgi, F.M. Preliminary report on severe acute respiratory syndrome coronavirus 2 (SARS-CoV-2) Spike mutation T478K. *Journal of medical virology* **2021**, *93*, 5638-5643.
27. Goher, S.S.; Ali, F.; Amin, M. The Delta Variant Mutations in the Receptor Binding Domain of SARS-CoV-2 Show Enhanced Electrostatic Interactions with the ACE2. *Medicine in drug discovery* **2021**, 100114.
28. Zeng, C.; Evans, J.P.; Qu, P.; Faraone, J.; Zheng, Y.-M.; Carlin, C.; Bednash, J.S.; Zhou, T.; Lozanski, G.; Mallampalli, R.; et al. Neutralization and Stability of SARS-CoV-2 Omicron Variant. *bioRxiv* **2021**, 2021.2012.2016.472934.
29. Chen, J.; Wei, G.-W. Omicron BA.2 (B.1.1.529.2): high potential to becoming the next dominating variant. *ArXiv* **2022**, arXiv:2202.05031v05031.
30. Kannan, S.R.; Spratt, A.N.; Sharma, K.; Sönnerborg, A.; Apparsundaram, S.; Lorson, C.; Byrareddy, S.N.; Singh, K. Complex Mutation Pattern of Omicron BA. 2: Evading Antibodies without Losing Receptor Interactions. **2022**.
31. COVID-19 subvariant XE: What to know. Available online: https://www.foxnews.com/health/covid-19-subvariant-xe-ba-2-coronavirus-pandemic (accessed on May 10, 2022).